Using MEMS mirrors to pattern electrical forces

Steven L. Neale*, Hsan-Yin Hsu, Justin K. Valley, Arash Jamshidi, Ming C. Wu
Berkeley Sensor and Actuator Center (BSAC) and Electrical Engineering and Computer Sciences
Dept., University of California, Berkeley, CA, 94720

ABSTRACT

By switching between two tilt angles MEMS mirrors can be used to produce spatial light patterns. This enables the Digital Micromirror Display (DMD, Texas Instruments) chip to produce the images found in some data projectors. In this paper we will show how these images can be converted into electrical patterns. We use the electrical gradients in these patterns to control the movement of particles through dielectrophoresis. We show how this can be used to move cells within PBS solution and characterize our device. We also discuss possible ways to improve our optical setup through Adaptive Optics (AO).

Keywords: Microelectromechanical Systems (MEMS), Micromanipulation, DMD, HeLa cells

1. INTRODUCTION

Optoelectronic tweezers (OET) use the selective illumination of a photoconductive layer to create areas of higher conductivity which are then thought of as 'virtual electrodes'. A liquid layer is sandwiched between the photoconductive layer which is deposited on ITO glass and a second ITO glass substrate. The illuminated pattern then controls the pattern of electrical fields within the liquid as shown in figure 1. The electrical gradients that are found at the edges of the optical pattern are then used to manipulate colloidal particles through dielectrophoresis. OET was first demonstrated with amorphous silicon [1,2,3,4] as the photoconductive layer, however this limits the range of conductivities that can be used for the suspending liquid (see section 1.1). Although cells have been manipulated by suspending them in an isotonic sugar solution of low conductivity it is desirable to keep them suspended in physiological buffer solution to increase cell viability and lengthen the time the cell can be kept healthy whilst being experimented on.
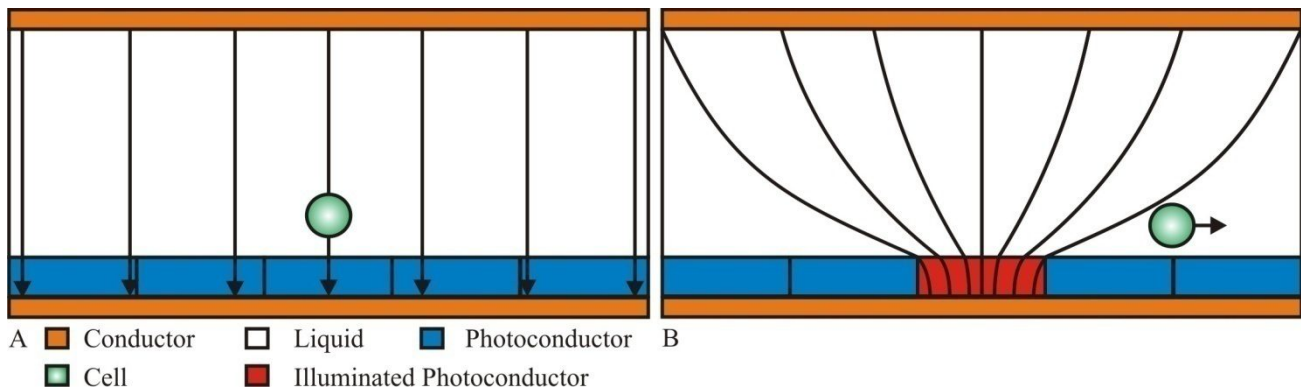

Fig. 1. A) An AC voltage is placed across the two conductive layers producing an electrical field as indicated by the electrical field lines (arrows). B) When a small area is illuminated the electrical field is concentrated in this area producing an electrical field gradient which causes the repulsion of the particle. This diagram shows the photoconductor split into discreet areas or pixels which is necessary in photo-transistor based OET to limit the diffusion of the charge carriers created.
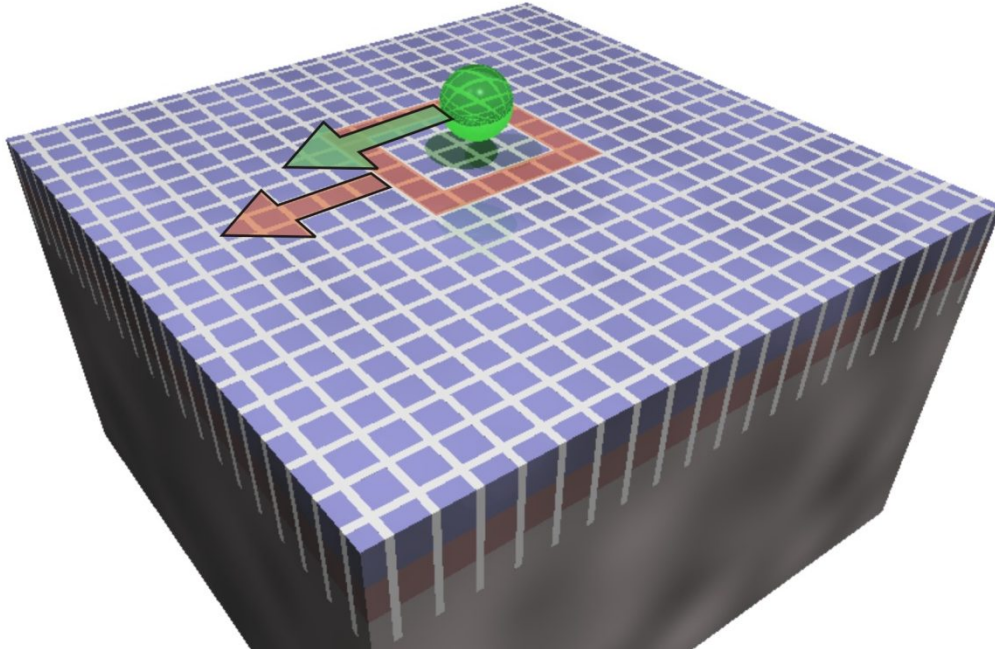
Fig. 2. A Ph-OET device is shown consisting of two layers of doped silicon which is etched into the pixilated pattern. The device can be illuminated with a square ring of light surrounding the cell to be trapped. The ring can then be moved causing the cell to move as indicated by the arrows.

To achieve this we have developed a phototransistor-based device (5) which in this paper we will characterize by measuring the force experienced by cells at different positions within the trap.

There are two ways in which Adaptive Optics (AO) could be used to enhance this device. By placing the Deformable Mirror between the projector that creates the device and the microscope objective the image focused onto the device could be corrected for the aberrations caused by the microscope such as spherical aberrations. The other possibility is that the effect of a layer of cells on top of the device could be mitigated through AO. It is often desirable to pattern the electrical fields in busy samples such as a device with a layer of cells covering the photoconductor that would distort the optical pattern. AO could be used to lessen the degradation of the optical image this causes (see section 5).

1.1 Phototransistor-based Optoelectronic Tweezers (Ph-OET)

Optoelectronic Tweezers (OET) use the conductivity change of the illuminated region of a photoconductive layer to act as a virtual electrode. Figure 2 shows how illuminating just a small area of the photoconductor concentrates the electrical field in the liquid just above this area.

This translates the optical pattern into an electrical pattern. When a polarizable particle is placed into an electrical field gradient it experiences a force called dielectrophoresis which arises from the force on each side of the dipole created within the particle being unequal. This force is given by;

$$F = 2\pi r^3 \varepsilon_m \, \mathrm{Re}[k(\omega)] \nabla E^2 \qquad (1)$$

Where r is the radius of the particle, ε_m is the permittivity of the medium, Re[k(ω)] is the real part of the Clausius-Mossotti factor and ∇E^2 is the gradient of the electrical field squared. This force can be either positive, towards the area of higher electrical field, or negative, towards the area of lower electrical field depending on the sign of the Clausius-Mossotti factor (figure 1 shows the case of negative dielectrophoresis). This factor is calculated from the relative permittivities of the particle and the liquid it is suspended in. For a cell the calculation of the Clausius-Mossotti factor is complicated by the cells heterogeneous constituents. A simple single shell model that describes the cell as a thin insulating membrane covering a conductive core gives good agreement between calculated and observed forces [6,7].

The experiments in this paper use a highly conductive medium which causes the cells to experience negative dielectrophoresis. Therefore to trap the cell a square pattern is illuminated around it.
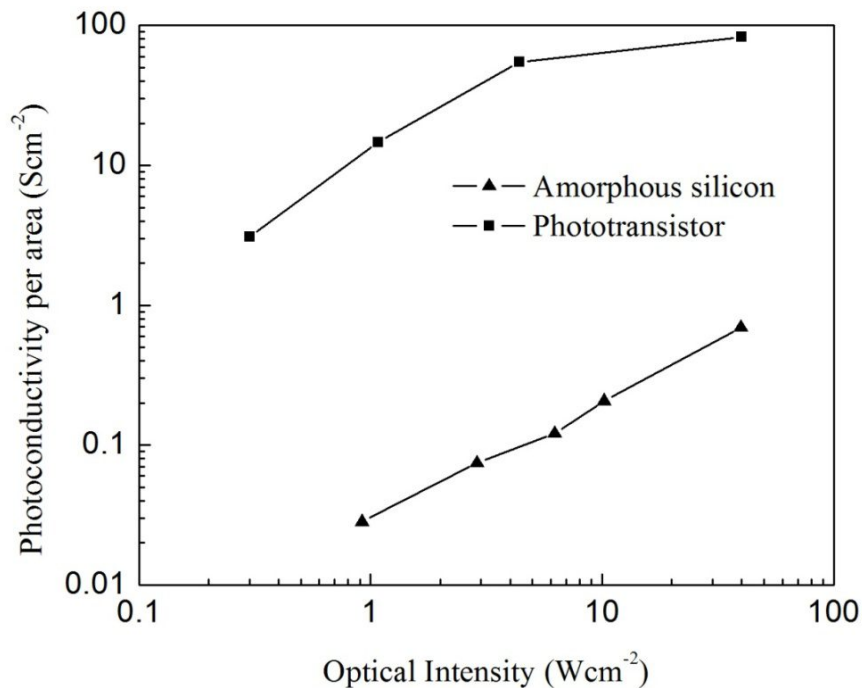

Fig. 3. The photoconductivity of the phototransistor is plotted (squares) as a function of optical intensity and compared to amorphous silicon (triangles) showing a higher conductivity for the same optical power.

To achieve the high electric field gradients that result in high forces (see Equation 1), we need the impedance of the photoconductive layer when dark to be higher than that of the cell suspension medium and the impedance of the illuminated region to be lower than the medium. This ensures that the majority of the electrical potential is dropped across the photoconductor when the device is dark and across the liquid when it is illuminated. If the impedance of the liquid is lower than the impedance of the illuminated photoconductor then the majority of the potential is dropped across the photoconductor reducing the potential drop within the liquid and hence reducing the electrical field within the liquid and the field gradients created. For this reason it is challenging to create strong forces in conductive liquids and to achieve this we have developed a phototransistor to replace the amorphous silicon that has been used in previous devices. The phototransistor provides a higher illuminated conductivity than amorphous silicon (see figure 3) and is designed to allow trapping in physiological buffer solution that has conductivity $1Sm^{-1}$.
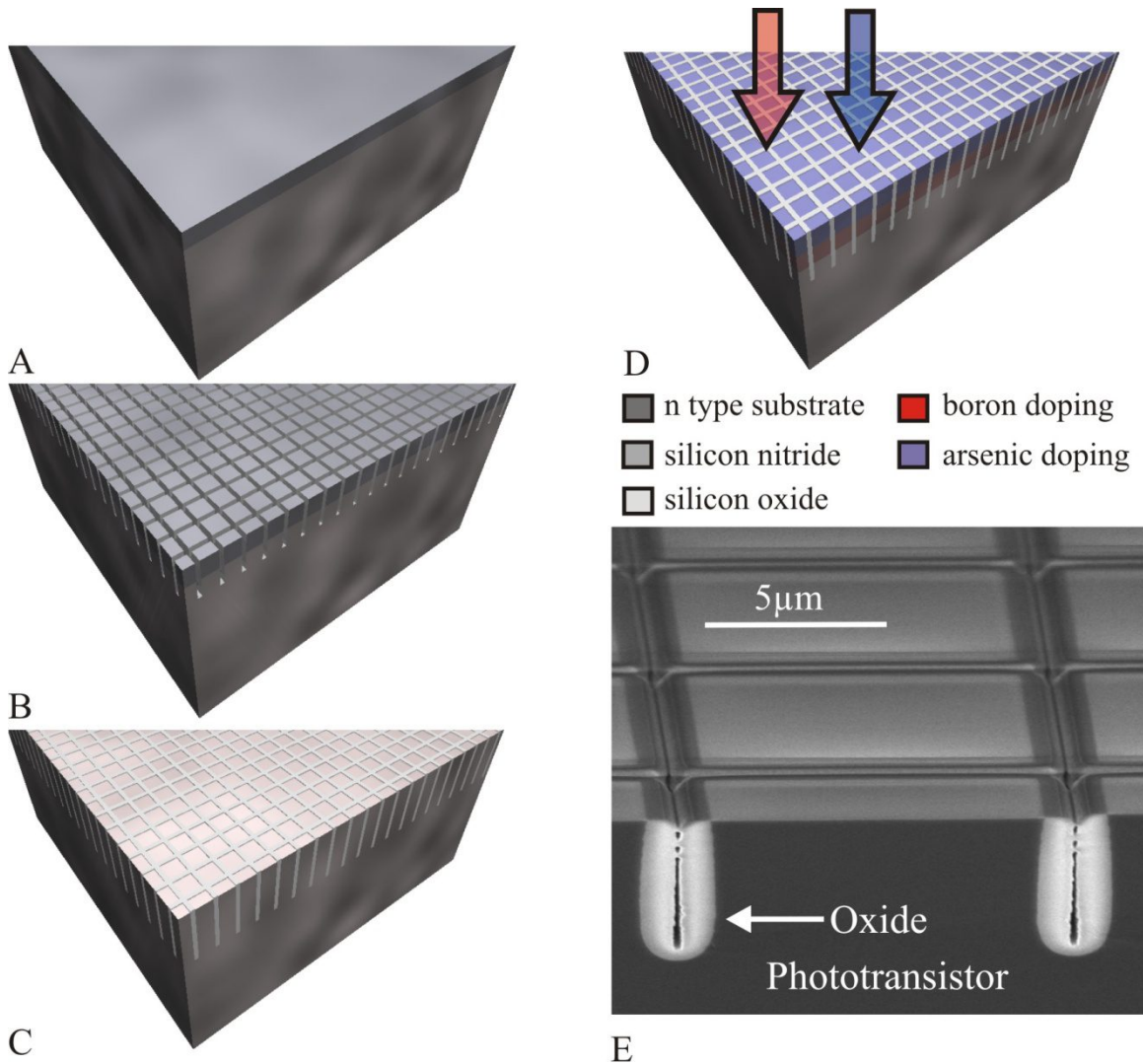
2. FABRICATION

Fig. 4. A Ph-OET device is fabricated from a silicon wafer that has A) nitride deposited onto it, B) pixels are patterned into it by photolithography and reactive ion etching (RIE), C) thermal oxide is grown in the gaps and the nitride is removed, D) a phototransistor created by implantation of boron and arsenic. E) Shows an SEM image of the finished device.

The Phototransistor based OET device was fabricated from a highly doped silicon substrate that had 5μm epitaxial silicon grown onto it with light n-doping to act as the collector of the phototransistor. A silicon nitride layer was then deposited onto this and photo resist was patterned onto this by photolithography. The resist was then used as a mask to etch through the nitride with reactive ion etching (RIE) and the nitride was used as a mask to etch into the silicon substrate using deep reactive ion etching (DRIE). Thermal silicon oxide is then grown in the gaps left by the etching and the nitride layer is stripped off. The phototransistor is then created by doping with boron to create the p-type layer and arsenic to create the n-type layer.

After the device has been fabricated a droplet of a few micro liters of solution containing the cells is placed onto the device and an ITO coated cover slide is placed on top of the device with tape acting as a spacer. The AC voltage is placed between this ITO layer and the conductive highly doped silicon substrate.

3. THE OPTICAL SETUP

The Ph-OET optical setup is a microscope constructed of the 30mm rail system from Thorlabs as shown in diagram 5. The light pattern is created by a DMD based projector (MP2400, Dell) with its projection lens removed. The pattern is reduced in size through a telescope and then reflected from a dichroic mirror (FD1C Cyan dichroic, Thorlabs) which reflects light above 575nm and transmits light of shorter wavelength. The pattern is then focused onto the device through a 20x long working distance objective (N.A. 0.42, Mitutoyo).

Fig. 5. The optical setup used for the Ph-OET experiments is a microscope as shown here. The optical pattern generated by a data projector is focused onto the chip through a 20x objective. The chip is also illuminated by a fiber illuminator which excites the fluorescence from the cells.

A fiber illuminator with a metal halide lamp (X-Cite 120 series) is used to excite the fluorescence from the. The light from this passes through a Kohler illumination path which gives control of the intensity and the field of the illumination by varying the size of the apertures. As this passes through the two dichroic mirrors and the light from the data projector is reflected by the first dichroic the fluorescence can be viewed by the CCD camera even though the light from the data projector is much brighter and would otherwise obscure this signal. A 50:50 beam splitter can be added between the fluorescence dichroic and the projector dichroic to add bright field illumination of the sample but this was not used for these experiments.

Before the experiments were performed, HeLa cells were dissociated with trypsin and re-suspended in DMEM cell culture with 10% FBS. Calcien-AM in DMSO (Molecular Probe) vital dye was introduced with final concentration of 5uM, and the cells were incubated in room temperature for 10mins. The resulting cells show green fluorescence with standard 488nm blue excitation.

4. RESULTS

To characterize the device described in this paper, experiments were carried out where a motorized stage is used to move the Ph-OET device with respect to the light pattern. This places a drag force on the cell being trapped which is countered by the trapping force of the optoelectronic tweezers. As the stage is moved back and forth the trapped particle moves within the trap whilst particles outside the trap are free to follow the stage (see figure 6). By increasing the velocity of the stage we can increase the force on the particle and force it to move further from the trap centre. As the trapping force must exactly match the drag force for the particle to remain in the trap calculating the drag force gives us a powerful tool to map out how much force the particle experiences at different position within the trap.
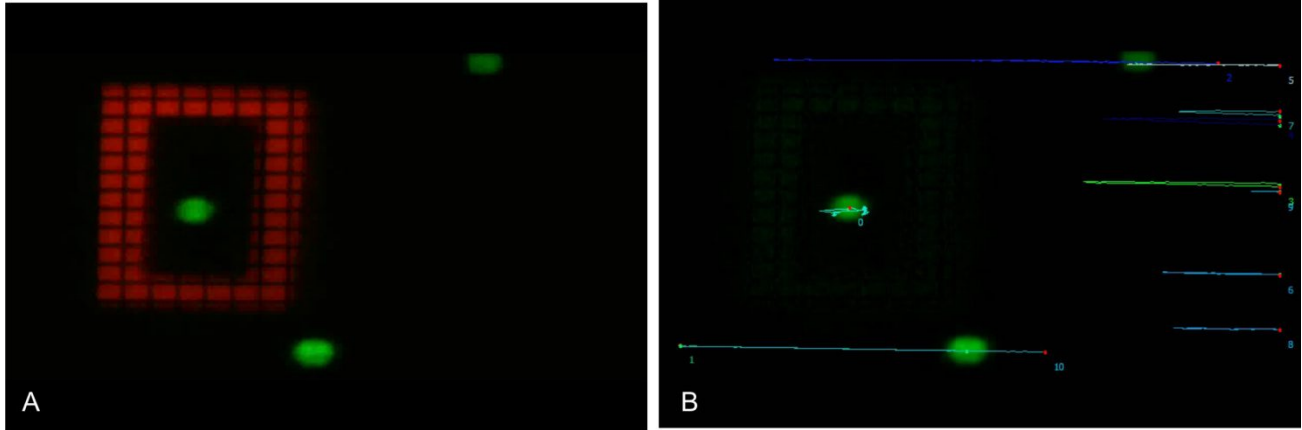
Fig. 6. A) Shows the first frame of a movie taken as the stage is moved right and left. The cells can be seen due to their green fluorescence and the red pattern is visible illuminating the pixilated photoconductor. B) Shows the same frame with the red part of the image removed by digital enhancement and the trajectories of the cells plotted. The cell within the trap has had its movement constricted whilst the cells outside the trap have been free to move with the stage.

It was found that to keep the cell within the trap it was necessary to have a dark area within the trap of at least four pixels wide. This is due to the repulsive force also having a vertical component that pushed the cell up and out of the trap if the dark area is reduced to three pixels or less. This is a key parameter for the trapping stiffness achievable as it provides the small size limit of the trap. The width of the illuminated ring was kept at 2 pixels wide so that as the device moves with respect to the light pattern one pixel is always fully illuminated.
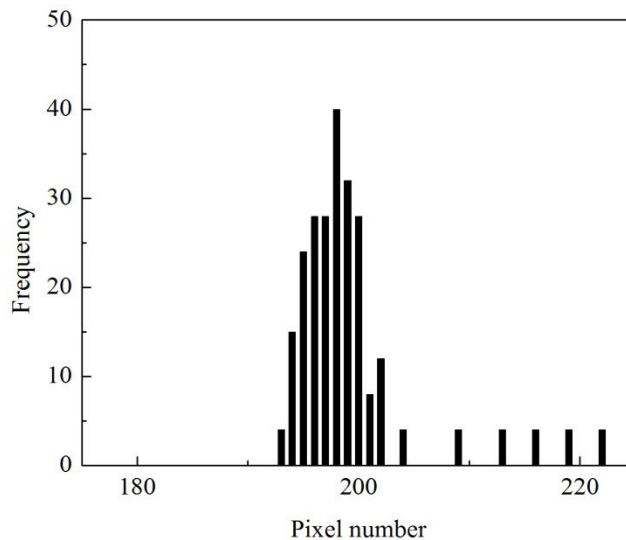

Fig. 7. The tracking software returns the position of the centre of the particle in pixels which is here plotted against pixel number for the case of the 7pixel wide trap at $20\mu ms^{-1}$ in the positive direction.

The pixilated nature of the device causes the particle to fluctuate in position within the trap as the stage is moved with respect to the light pattern. This, along with the surface roughness of the device, causes the position of the particle to form a distribution about the mean trapping position. Figure 7 shows this distribution. Here the frequency with which the centre of the particle was found at each pixel is plotted against the number of that pixel. This shows a roughly Gaussian distribution from which a FWHM of 2.8 microns can be calculated. This is a useful measure of how much the particle moves whilst being trapped and can be used as a measure of the uncertainty of the position of the particle.
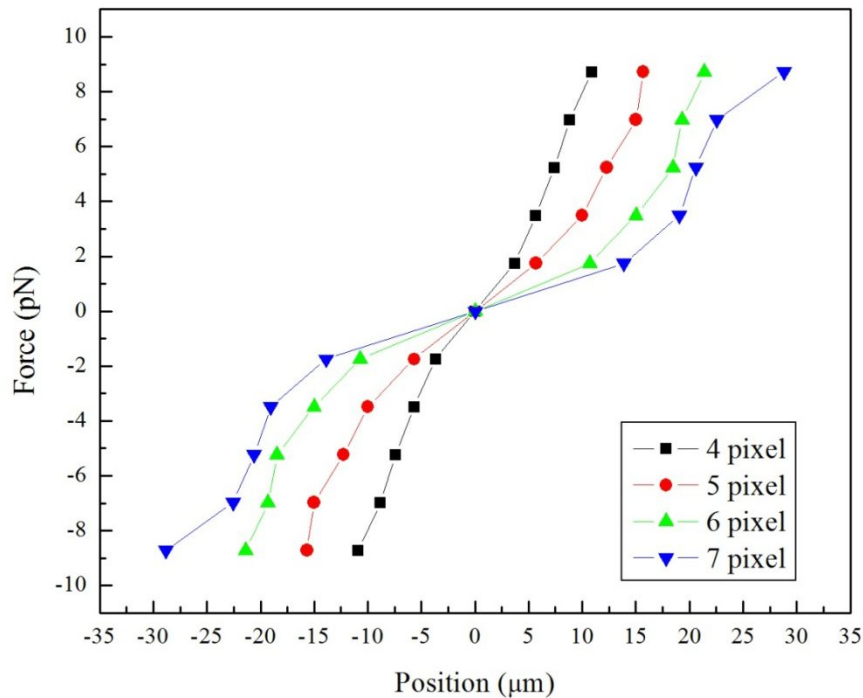
Fig. 8. The mean position of the particle is plotted against the force on the particle during each experiment. The four pixel wide trap has the greatest stiffness and is closest to the ideal case where the force is proportional to the distance from the trap centre.

The width of the trap was then varied from 4 dark pixels to 5, 6 and 7 dark pixels wide and the trap stiffness measured for each pattern. The particle tracking software [8] used relies on the pattern matching ability of LabVIEW so that a shape that is defined in the first frame of the video is tracked in each subsequent frame and returns the coordinates of the centre of the particle in pixels.

The A.C. voltage used in these experiments was 10V peak to peak at 2 MHz supplied by a function generator. In each case the maximum trapping velocity was found to be 20μms^{-1} giving a force of 8.7pN. The trap diameter is defined as the distance between the position of the centre of the cell when moving the trap in one direction at this maximum velocity and its position when the direction is reversed. This was found to be 24μm for the 4 pixel wide trap, 31 μm for the 5 pixel wide trap, 43 μm wide for the 6 pixel wide trap and 58 μm wide for the 7 pixel wide trap. This gives a trap stiffness for the 4 pixel wide trap of 8.38x10^{-7} Nm^{-1}. The four pixel wide trap has a profile closest to the linear case where force is proportional to distance for the trap centre so it makes sense to calculate this average stiffness for this trap. However as the trap becomes larger the profile becomes more nonlinear and so this measurement becomes less appropriate. Here the force increases more strongly as the particle moves away from the centre of the trap and the stiffness increases. This low stiffness in the centre of the trap means a small force can move the particle a long distance from the trap centre showing that the four pixel wide trap is the preferable choice for cell movement. The interesting aspect of these results is that the smallest trap is as close to linear as it is showing that an almost ideal trap profile can be created even with a Ph-OET pixel size as large as 10.35μm.

Previous work has shows that an OET device with an a-Si photoconductor can produce traps with stiffness of 3×10^{-6} Nm^{-1} for HeLa cells in a 10mSm^{-1} isotonic sugar solution [9]. These traps produce positive DEP allowing the particle to be moved at 50μms^{-1} with a trap diameter of just 12μm. To compare how well this device would work with high conductivity media we tried cells in 100mSm^{-1} media, an order of magnitude more conductive, and found the maximum velocity the cell could be moved at was 4μms^{-1}. If the force reduces by as much when we increase the conductivity by another order of magnitude, to the conductivity of PBS, the force would be over 2 orders of magnitude smaller than at 10mSm^{-1}(we can't measure this as the forces are too small). This would make the phototransistor based device over 25 times stiffer at this conductivity.

5. ADAPTICE OPTICS (AO) AND OET

It would be possible to improve upon our current OET device by integrating AO into the optical setup. This could help to improve the quality of the optical image projected onto the photoconductive layer. This image can be distorted by either the systematic aberrations introduced by the microscope such as spherical aberration (the image is focused by several spherical lenses before it passes through the objective, see section 3) or by the particles being manipulated. In a busy sample there may be many particles that cause time varying errors in the image projected by refracting it before it hits the photoconductive surface see figure 9.
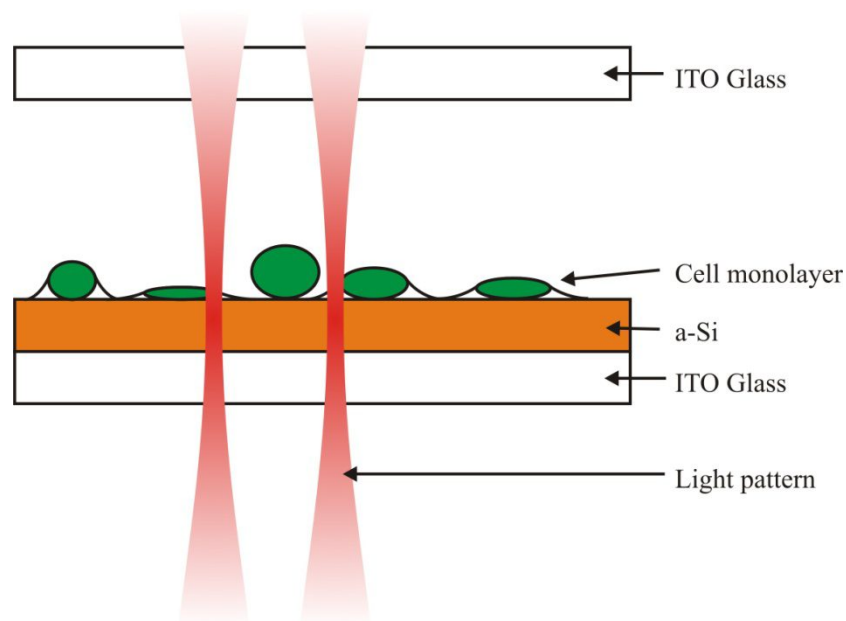

Fig. 9. Particles such as the cells shown in this figure may interact with the light, which enters from the top, before it reaches the photoconductive substrate. It may be possible to use AO to correct for the errors this produces.

To implement this approach a laser beam to act as a "guide star" could be focused through the optical setup, the perturbation of which would be sensed with a wave front sensor and the resulting corrections would be fed back to the deformable mirror which would be placed after the projector in the optical setup.

6. CONCLUSION

In this paper we show how it is possible to move cells in PBS through the patterning of electrical fields which are controlled by the optical patterns created by a MEMS mirror based device. We show that the high conductivity of the PBS solution requires the use of a photo-transistor as the photoconductive layer of the device. We characterize the traps created by this device and measure a trap stiffness of 8.38×10^{-7} Nm^{-1}. We also consider how AO could be used to improve our device by removing aberrations in the images being projected onto the photo-transistor due to imperfections in the microscope or by particles in the OET device.

REFERENCES

[1] Chiou, P. Y., Ohta, A. T., and Wu, M. C., "Massively parallel manipulation of single cells and microparticles using optical images," Nature 436, 370-372 (2005).

[2] Chiou, P. Y., Ohta, A. T., and Wu, M. C., "Toward all optical lab-on-a-chip system: optical manipulation of both microfluid and microscopic particles," Proceedings of the SPIE, Volume 5514, 73-81 (2004).

[3] Ohta, A. T., Chiou, P. Y., Phan, H. L., Sherwood, S. W., Yang, J. M., J. M., Lau, J. M., Hsu, H. Y., Jamshidi, A., and Wu, M. C., "Optically controlled cell discrimination and trapping using optoelectronic tweezers," IEEE Journal of Selected Topics in Quantum Electronics 13, 235-243 (2007).

[4] Ohta, A. T., Chiou, P. Y., Han, T. H., Liao, J. C., Bhardwaj, U., McCabe, E. R. B., Yu, F., Sun, R., and Wu, M. C., "Dynamic Cell and Microparticle Control via Optoelectronic Tweezers," Microelectromechanical Systems, Journal of 16, 491-499 (2007).

[5] Hsu, H. Y., Ohta, A. T., Chiou, P. Y., Jamshidi, A., and Wu, M. C., "Phototransistor-based optoelectronic tweezers for cell manipulation in highly conductive solution," in TRANSDUCERS '07 & Eurosensors XXI 14th International Conference on Solid-State Sensors, Actuators and Microsystems. Lyon, France, 2007.

[6] Hughes, M.P., Nanoelectromechanics in engineering and biology, CRC Press (2003).

[7] Neale, S. L., Mazilu, M., Wilson, J. I. B., Dholakia, K., and Krauss, T. F., "The resolution of optical traps created by light induced dielectrophoresis (LIDEP)," Optics Express 15, 12619-12626 (2007).

[8] StAT particle tracking software created by Milne G, http://faculty.washington.edu/gmilne/tracker.htm

[9] Neale, S.L., Ohta, A.T., Hsu, H.Y., Valley, J.K., Jamshidi, A., and Wu, M.C., "Trap profiles of projector based optoelectronic tweezers (OET) with HeLa cells", paper in preparation.